www.czasopisma.pan.pl PAN www.journals.pan.pl
Opto-Electronics Review 26 (2018) 201–209

Contents lists available at ScienceDirect

Opto-Electronics Review

journal homepage: http://www.journals.elsevier.com/opto-electronics review

Full Length Article

Study of the Light Emitting Diode as a photoreceptor: Spectral and electrical characterization as function of temperature and lighting source

E. Vannacci [a], S. Granchi [a,*], M. Cecchi [a], M. Calzolai [a], E. Mazzi [b], E. Biagi [a]

[a] Department of Information Engineering (DINFO), University of Florence, Via Santa Marta, 3, 50139, Florence, Italy
[b] Power Pure Control s.r.l., Via Carbonia, 2, 56021, Navacchio, Pisa, Italy

ARTICLE INFO

Article history:
Received 30 January 2018
Received in revised form 17 May 2018
Accepted 7 June 2018
Available online 30 June 2018

Keywords:
Light emitting diode
Photovoltaic effect
Current voltage characteristic
Photodetector
Junction temperature
Spectral analysis

ABSTRACT

In this study, the temperature influence on the spectral responsivity of a Light Emitting Diode (LED) used as a photoreceptor, combined to light source spectrum is correlated to electrical characteristics in order to propose an alternative method to estimate LED junction temperature, regardless of the absolute illumination intensity and based on the direct correlation between the integral of the product of two optical spectra and the photo-generated currents. A laboratory test bench for experimental optical measurements has been set in order to enable any characterizing of photoelectric devices in terms of spectral behaviour, in a wavelength range placed between 400–1000 nm, and of current-voltage characteristics as function of temperature by using two different illumination sources. The temperature is analysed in a range from 5 °C up to 85 °C, so as to evaluate thermal variation effects on the sensor performance. The photo-generated current of two LEDs with different peak wavelengths has been studied. Research has observed and mathematically analysed what follows: since the photo-generated current strictly depends on the combination between the spectral response of the photoreceptor and the lighting source response, it becomes possible to estimate indirectly the junction temperature of the LEDs by considering the ratio between the photogenerated currents obtained by using two different illumination sources. Such results may for one thing increase knowledge in the fields where LEDs are used as photo-detectors for many applications and for another, they could be extended to generic photodetectors, thus providing useful information in photovoltaic field, for instance.

1. Introduction

When aiming at increasing the photoreceptor performance, such as a solar cell, it is important to study the impact of temperature on the generated photocurrent [1–3], together with the spectral response changes [4–8]. Since 1980 s, some researchers [9,10] have investigated in this field, in order to determine the dominant factors influencing efficiency at elevated temperatures [11,12]. It is noted that the more the temperature increases, the more the short circuit current density (J_{sc}) grows [4–8] and theoretical models have been developed to support this dependence [8,13,14].

As we know, there is a significant dependence of the bandgap energy in semiconductor on junction temperature T: as temperature increases, bandgap energy decreases, producing both a shift of the emission and absorption spectra towards higher wavelenghts (lower energy) [6].

Actually, a complete characterization of the photo-detector's behaviour should take into account the source optical spectra and the absorption spectra as temperature functions.

This paper presents results on the characterization of photodetectors, by considering the different matching between source and absorption spectra as the receiver's temperature changes. A practical solution to carry out the study has focussed on using Light Emitting Diodes (LEDs) as a bandwidth-limited photo-detector. Their narrow absorption bandwidth [15–17] combined with the different wavelength ranges has allowed selecting different mutual overlaps between source and absorption spectra.

In literature, studying LED as a photoreceptor had initially a very limited scope, namely characterizing the dependence of junction temperature on the internal efficiency [18] in order to investigate materials for LED construction, thus increasing optical

* Corresponding author at: Ultrasound and Non-Destructive Testing Lab, Department of Information Engineering (DINFO), University of Florence, via Santa Marta 3, 50139, Florence, Italy.
E-mail addresses: enrico.vannacci@unifi.it (E. Vannacci), simona.granchi@unifi.it (S. Granchi), mattia.cecchi@stud.unifi.it (M. Cecchi), marco.calzolai@unifi.it (M. Calzolai), emanuele@purepowercontrol.com (E. Mazzi), elena.biagi@unifi.it (E. Biagi).

https://doi.org/10.1016/j.opelre.2018.06.001
1230-3402/

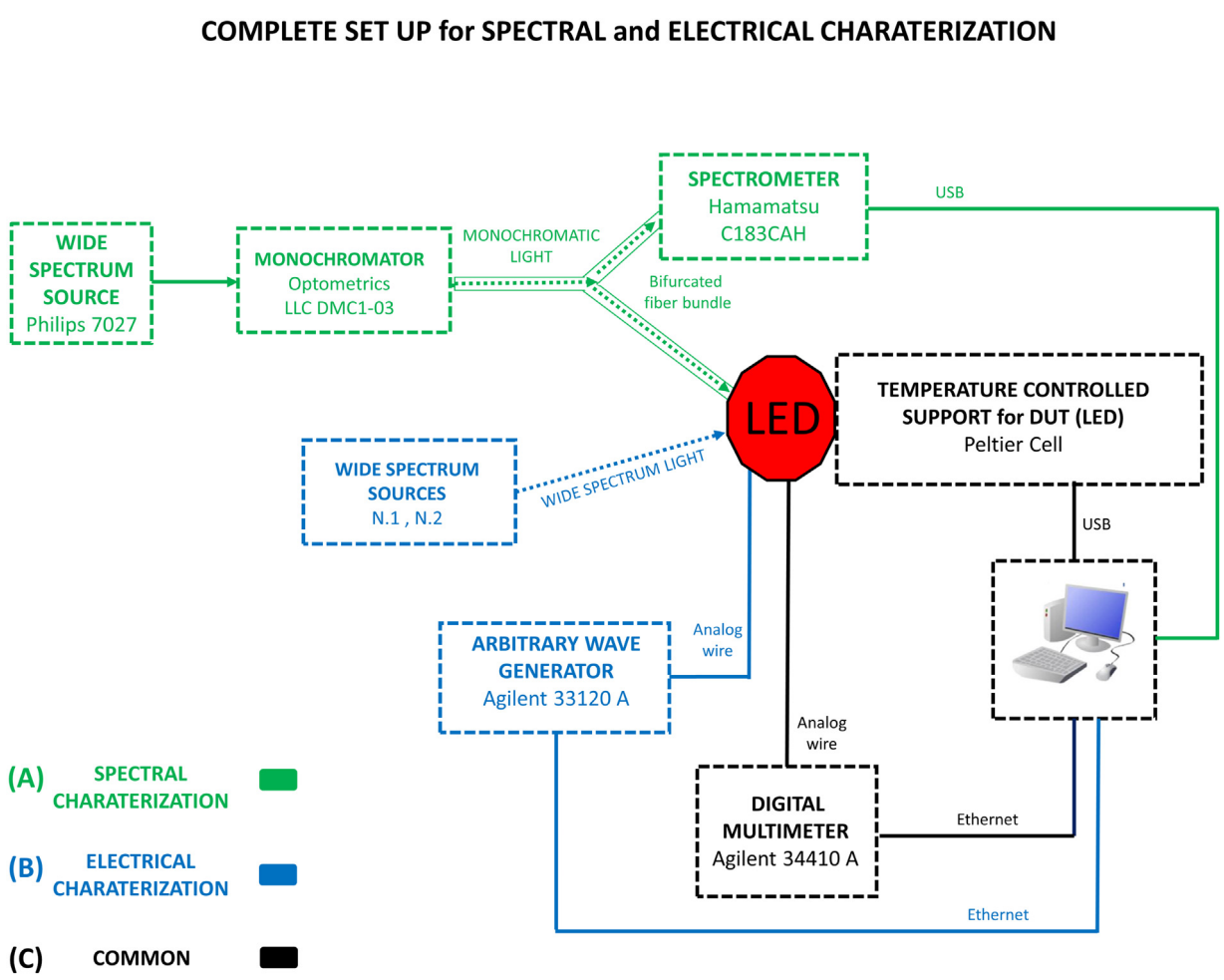

Fig. 1. Scheme of the measurement bench for inverse spectral and electrical LED characterization. The green and black blocks are involved in the spectral characterization, while the blue and black blocks in the electrical characterization.

performances [19–22] or when exploiting LED as a sun photometer [23–27]. On the other hand, recently, the dual LEDs functioning has been largely analysed and exploited within many other new and interesting applications [28–32], such as two-way communication systems [33–35], as colour sensing and illumination devices, as photo-detector in the biomedical field [36,37], and also as field radiometers [38,39].

The current study presents results which may improve knowledge in this emerging field; moreover, it provides the user with a full characterization of LEDs' inverse functioning that is not available in the technical paperwork.

A complete test bench has been set in order to perform, at the same time, spectral and electrical characterization of the optical devices used as light detectors, as temperature changes.

Two different LED models have been analysed to measure absorption spectra and current-voltage characteristics in the fourth quadrant, at five different temperature values and with two different light sources.

Junction temperature is one of the key parameters in LED applications and it has been extensively studied in literature. In particular, in Ref. [40] the junction temperature has been evaluated by measuring the LED inverse current. In this work a novel method to evaluate LED junction temperature is suggested. LED junction temperature has been estimated by measuring a short circuit photocurrent ratio measured on the analysed device and illuminated by two different sources. This technique allows for temperature assessment regardless of the source's illumination intensity.

2. Materials and methods

2.1. LED spectral characterization

Authors have spent their efforts to define an experimental measurement system able of performing repeatable, representative and reliable measurements, where multiple parameters can be controlled and varied at once. As to the inverse characterization, an appropriate measurement bench, schematically reported in Fig. 1, has been set. The green and black blocks in the measurement chain of the Fig.1 represent the instrumental components used to analyse the absorption spectrum of the LED employed as a photoreceptor. The optical equipment consists of:

1 A wide spectrum halo source, Philips 7027, with a nominal power of 50 W;
2 A monochromator (Optometrics LLC DMC1-03) with a range of 300–850 nm that selects a narrow (3 nm at -3 dB) spectrum light, which is guided, through an optical fiber bundle, towards LED to be characterized. In this experimentation the monochromator range has been modified to enlarge its wavelength range up to 1000 nm;
3 A 6.5 digit Multimeter Agilent 34410 A which allows for any measuring of voltage or current with high accuracy;
4 A Peltier cell performing a temperature control from 5 °C up to 85 °C and allowing for the analysis of the LED behaviour at

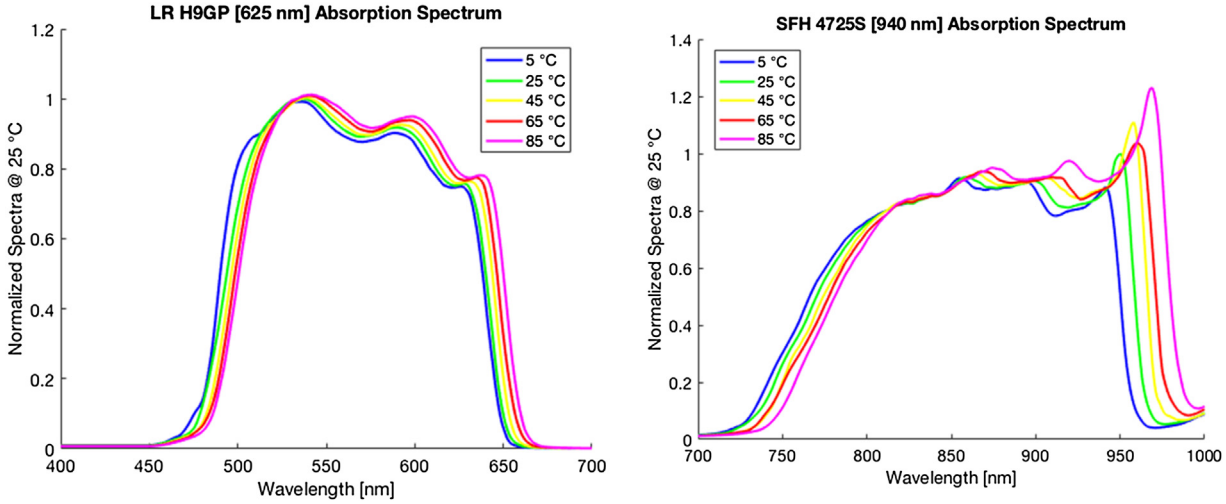

Fig. 2. Absorption normalized spectra at different temperature values for red LED (LR H9GP on the left) and LED (SFH 4725S on the right). As temperature increases, the spectrum shifts towards longer wavelengths.

different temperature levels. A software-dedicated PC interface controls the cell settings;

5 The spectrometer Hamamatsu C183CAH having a wavelength range of 400–1000 nm is used to acquire and analyse the light, guided into it through an optical fiber.

Each monochromatic light selected by means of the monochromator is carried, through a bifurcated fiber bundle, both to the DUT and into the spectrometer which evaluates the relative power spectral distribution. The photogenerated current at the output of the DUT is measured by multimeter. Data coming out from the multimeter and from the spectrometer are managed, saved and processed by a dedicated software, developed in Matlab environment in order to reconstruct the absorption spectrum.

All the measurements have been executed on an optical table (PTM11108, Thorlabs Inc., New Jersey, USA).

2.2. LED electrical characterization

Measurements of current-voltage (I–V) characteristics have been carried out on the basis of the same diagram shown in Fig. 1, but in this case, the used instrumentation is represented by the blue and black blocks and, as it is shown, the illumination of the LED is performed by directly using wide spectrum sources. The set up allows for the measurement of the Device Under Test (DUT) characteristics in all functioning quadrants, regardless of the used load. For each constant voltage level, generated by Agilent 33120 A, the corresponding device current output is measured through the multimeter and curves are acquired in Matlab environment on PC. Data acquisition by multimeter and software commands are synchronous. In the context of current study, measurements have been limited to the fourth quadrant, where the diode has a photovoltaic behaviour. The reason is grounded on what follows:

- the chosen LEDs present a diode for reverse-voltage protection, thus preventing a full characterisation due to reverse bias;
- all the data needed for the electrical analysis (short circuit photocurrents) are included in the fourth quadrant.

Two different measurement campaigns have been performed, with two different light sources. The first (source N.1) was a halogen lamp with 150 W power (Crouse Hinds 2011, USA), equipped with a dichroic lens which reduces strongly the reflected InfraRed (IR) light components; while the second (source N.2) was a wide spectrum halo source with a power of 60 W (Zeiss 380018, Germany).

For each measurements set, the current (I) and the voltage (V) values have been acquired at five different temperature values of: 5 °C, 25 °C, 45 °C, 65 °C, 85 °C. Among the several LED models studied, two devices have been chosen, so that their bandwidth composition covered the available wavelengths range (400–1000 nm). The chosen LEDs are produced by OSRAM Opto Semiconductors and belong to the OSLON Black Series, in short they are: the LRH9GP, red (emission peak at 625 nm), realized in InGaAlP and the SFH 4725S, infrared (emission peak at 940 nm), realized in GaAs. They presented the same physical packages, lenses and active areas (1 mm^2).

Finally, data have been processed in Matlab environment, with the aim to compare the performances of the analysed DUTs.

3. Results

As afore mentioned, spectral measurements have been executed in a wavelength range between 400 nm and 1000 nm, that being the calibration range of the spectrometer.

By using the setup of Fig. 1, the LEDs absorption spectra have been measured and represented in Fig. 2, according to the different temperature levels. The spectral shift is clearly visible for each LED model.

In order to highlight the correlation between the I–V characteristics of the LED, used as a photodetector, with a different overlapping between source and absorption spectra, greater attention has been paid in measuring and representing these curves in the fourth quadrant, as temperature changed and on the basis of the two different broadband light sources.

The I–V curves shown in Fig. 3 have been obtained by exploiting the source N.1, while as to the source N.2, the measured I–V characteristics are reported in Fig. 4.

In order to analyse the temperature dependence of the LEDs' electrical behaviour, the ratio R_{scc} (short circuit current ratio) between the short circuit photocurrent I_{sc} at two different temperatures T_1 and T_2 has been calculated:

$$R_{scc} = \frac{I_{sc}\big|_{T_1}}{I_{sc}\big|_{T_2}} \tag{1}$$

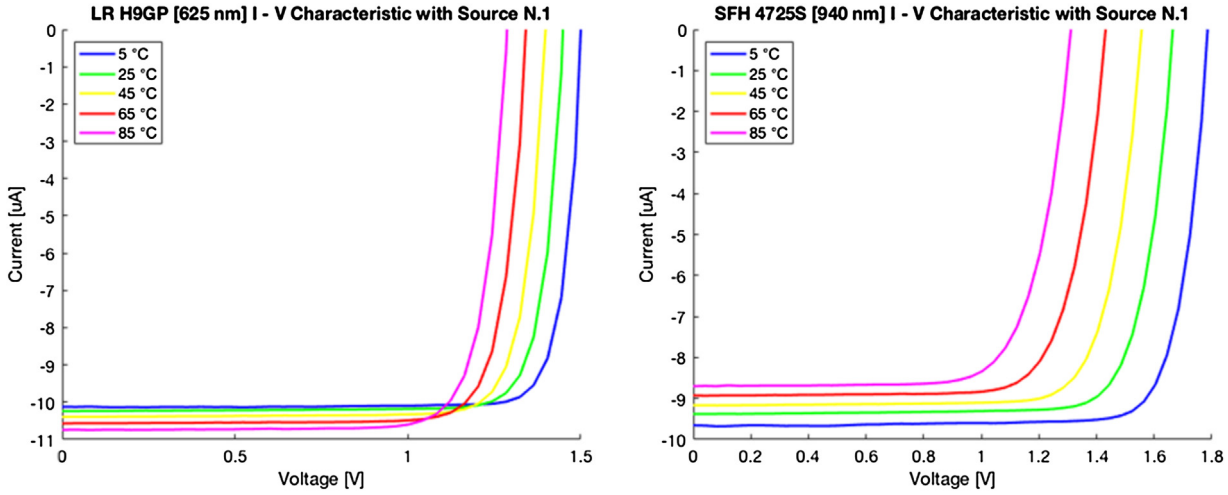

Fig. 3. I–V characteristics at different temperature values, for red LED (LR H9GP on the left) and for infrared LED (SFH 4725S on the right), illuminated by light source N.1. For red LED (LR H9GP) as the temperature is higher, the current (I_{sc}) increases and the voltage (V_{oc}) decreases. For infrared LED (SFH 4725S) as the temperature is higher, both the current (I_{sc}) and the voltage (V_{oc}) decrease.

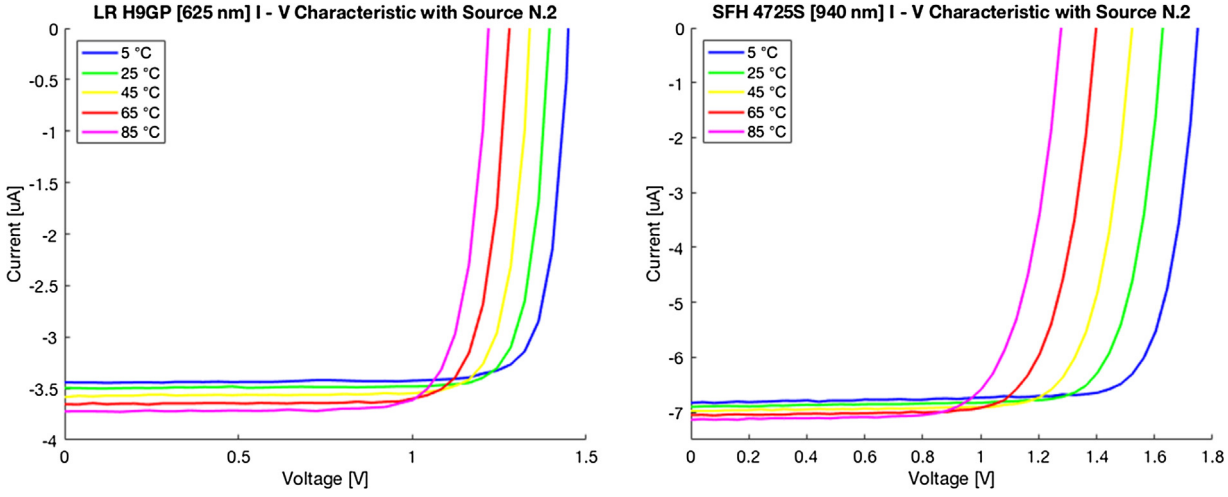

Fig. 4. I–V characteristics at different temperature values, for red LED (LR H9GP on the left) and for infrared LED (SFH 4725S on the right), illuminated by light source N.2. For both LEDs as the temperature is higher, the current (I_{sc}) increases and the voltage (V_{oc}) decreases.

On the other hand, in order to analyse the spectral behaviour while temperature changes, another ratio R_{sp} (spectral ratio) has been calculated as follows:

$$R_{sp} = \frac{\int_{\lambda_{min}}^{\lambda_{max}} S_i(\lambda)\, S_{LED}(\lambda)\big|_{T1} d\lambda}{\int_{\lambda_{min}}^{\lambda_{max}} S_i(\lambda)\, S_{LED}(\lambda)\big|_{T_2} d\lambda} \tag{2}$$

Where $S_i(\lambda)$ is the spectral power distribution of the i-th source used for spectral measurements, $S_{LED}(\lambda)$ is the measured absorption spectrum of a LED at a chosen temperature and λ_{min} and λ_{max} are defined by the measurement range and in this case they are equal, respectively to 400 nm and 1000 nm

An estimate of two ratios has been calculated for each temperature couple which has been examined, as reported in Table 1, where results are referred to each analysed LED correctly matched with the kind of source exploited.

As to each analysed LED, you could infer that the R_{scc} and R_{sp} parameters are highly superimposable on one another, which has been also corroborated by the mean [MEAN (R_{sp}/R_{scc})] and the standard deviation [STD (R_{sp}/R_{scc})] values of the ratio R_{sp}/R_{scc}, assessed for every source and LED. Furthermore, the mean value (MEAN_TOT = 0.998) of the ratio R_{sp}/R_{scc} and the standard deviation (STD_TOT = 0.008), calculated for any data, can prove the worthiness of such measurements.

Consequently, you can infer that:

$$R_{sp}\left(S_i, T_j, T_h\right) \cong R_{scc}(S_i, T_j, T_h) \tag{3}$$

with R_{sp} (S_i, Tj,T_h) : the spectral ratio calculated at T = Tj and T = T_h with the source S_i

R_{scc} (S_i, Tj,T_h): the short circuit current ratio calculated at T = Tj and T = T_h with the source S_i

I_{sci}: the short circuit current with the source S_i

That also is:

$$\frac{I_{sci}\big|_{T_h}}{\int_{\lambda_{min}}^{\lambda_{max}} S_i(\lambda)\, S_{LED}(\lambda)\big|_{T_h} d\lambda} \cong \frac{I_{sci}\big|_{T_j}}{\int_{\lambda_{min}}^{\lambda_{max}} S_i(\lambda)\, S_{LED}(\lambda)\big|_{T_j} d\lambda} \tag{4}$$

It follows:

$$I_{sci}(T) \propto \int_{\lambda_{min}}^{\lambda_{max}} S_i(\lambda) S_{LED}(\lambda, T)\, d\lambda \Longrightarrow I_{sci}(T)$$
$$= h_i \int_{\lambda_{min}}^{\lambda_{max}} S_i(\lambda) S_{LED}(\lambda, T)\, d\lambda \tag{5}$$

Table 1
Values of ratio R_{sp} (spectral ratio) and R_{scc} (short circuit current ratio) at different temperatures. T_1 and T_2: temperature.

T_1	T_2	LED LRH9GP				LED SFH4725S			
		Source N.1		Source N.2		Source N.1		Source N.2	
		R_{sp}	R_{scc}	R_{sp}	R_{scc}	R_{sp}	R_{scc}	R_{sp}	R_{scc}
5 °C	25 °C	0.996	0.988	0.996	0.985	**1.020**	**1.030**	0.982	0.990
	45 °C	0.980	0.974	0.976	0.960	**1.048**	**1.053**	0.971	0.979
	65 °C	0.960	0.957	0.953	0.942	**1.061**	**1.082**	0.968	0.969
	85 °C	0.939	0.942	0.930	0.924	**1.091**	**1.110**	0.955	0.957
25 °C	45 °C	0.984	0.986	0.980	0.975	**1.027**	**1.023**	0.989	0.990
	65 °C	0.963	0.969	0.957	0.956	**1.040**	**1.051**	0.986	0.979
	85 °C	0.943	0.953	0.935	0.938	**1.069**	**1.078**	0.973	0.967
45 °C	65 °C	0.979	0.983	0.977	0.981	**1.012**	**1.027**	0.997	0.989
	85 °C	0.959	0.967	0.953	0.963	**1.041**	**1.053**	0.984	0.977
65 °C	85 °C	0.979	0.984	0.976	0.981	**1.029**	**1.026**	0.987	0.988
MEAN(R_{sp}/R_{scc})		**0.998**		**1.003**		**0.991**		**1.001**	
STD(R_{sp}/R_{scc})		**0.006**		**0.008**		**0.007**		**0.006**	
MEAN_TOT (R_{sp}/R_{scc})		**0.998**							
STD_TOT (R_{sp}/R_{scc})		**0.008**							

MEAN(R_{sp}/R_{scc}), STD(R_{sp}/R_{scc}): mean and standard deviation values of R_{sp}/R_{scc}, evaluated for every source and LED.
MEAN_TOT (R_{sp}/R_{scc}), STD_TOT (R_{sp}/R_{scc}): mean and standard deviation values calculated over all data.

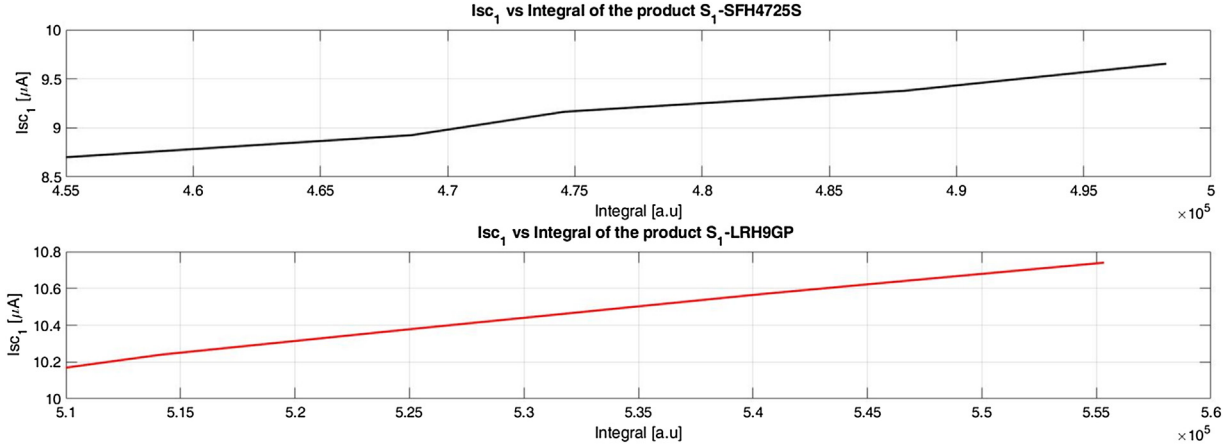

Fig. 5. Short circuit photo generated current I_{sc1} vs integral of the product between LED power absorption spectrum and power spectrum of source N.1.

With h_i: the proportional coefficient between $I_{sci}(T)$ and the corresponding integral.

In Fig.5 the short circuit current I_{sc1} is represented as a function of the integral of the product between absorption spectrum and Source N.1, for each DUT. As you would theoretically expect, results highlight the linear dependence of short circuit current from the corresponding values of the integral of the optical spectra's product.

In the following we explain the proposed method to estimate the junction temperature of DUTs based on measuring the ratio between the short circuit photocurrents I_{sc} obtained with two different sources.

Consider two sources whose power spectra $S_1(\lambda)$ and $S_2(\lambda)$ are expressed as follows:

$$\begin{aligned} S_1(\lambda) &= k_1(\lambda)A(\lambda) \\ S_2(\lambda) &= k_2(\lambda)A(\lambda) \\ A(\lambda) &= K\,S(\lambda) \end{aligned} \tag{6}$$

Where $S(\lambda)$ is a large bandwidth power spectrum, $k_1(\lambda)$ and $k_2(\lambda)$ represent the ratio between $S_1(\lambda)$ and $S_2(\lambda)$ in respect of $S(\lambda)$, respectively and K represents the illumination intensity.

Let be:

$$I_{SC1}(T) = h_1 K \int_{\lambda_{\min}}^{\lambda_{\max}} S(\lambda)\,k_1(\lambda)\,S_{LED}(\lambda, T)\,d\lambda \tag{7}$$

$$I_{SC2}(T) = h_2 K \int_{\lambda_{\min}}^{\lambda_{\max}} S(\lambda)\,k_2(\lambda)\,S_{LED}(\lambda, T)\,d\lambda \tag{8}$$

$$\frac{I_{SC2}(T)}{I_{SC1}(T)} = \frac{h_2 \int_{\lambda_{\min}}^{\lambda_{\max}} S(\lambda)\,k_2(\lambda)\,S_{LED}(\lambda, T)\,d\lambda}{h_1 \int_{\lambda_{\min}}^{\lambda_{\max}} S(\lambda)\,k_1(\lambda)\,S_{LED}(\lambda, T)\,d\lambda} \tag{9}$$

Define the ratio of I_{sc2} to I_{sc1} as a temperature function as follows:

$$\Gamma_{Isc}(T) = \frac{I_{SC2}(T)}{I_{SC1}(T)} \tag{10}$$

The function $\Gamma_{Isc}(T)$ turns out to be dependent on temperature, according to the variations of the ratio of the product's integral between sources spectra and LED absorption spectrum, regardless of illumination intensity.

Let:

$$\Gamma_{NIsc}(T) = \frac{I_{SC2}(T)/I_{SC2}\left(T_{ref}\right)}{I_{SC1}(T)/I_{SC1}\left(T_{ref}\right)} \tag{11}$$

the normalized ratio in respect of the two short circuit currents measured at the reference temperature (T_{ref}) that is considered to be 25 °C, in this case.

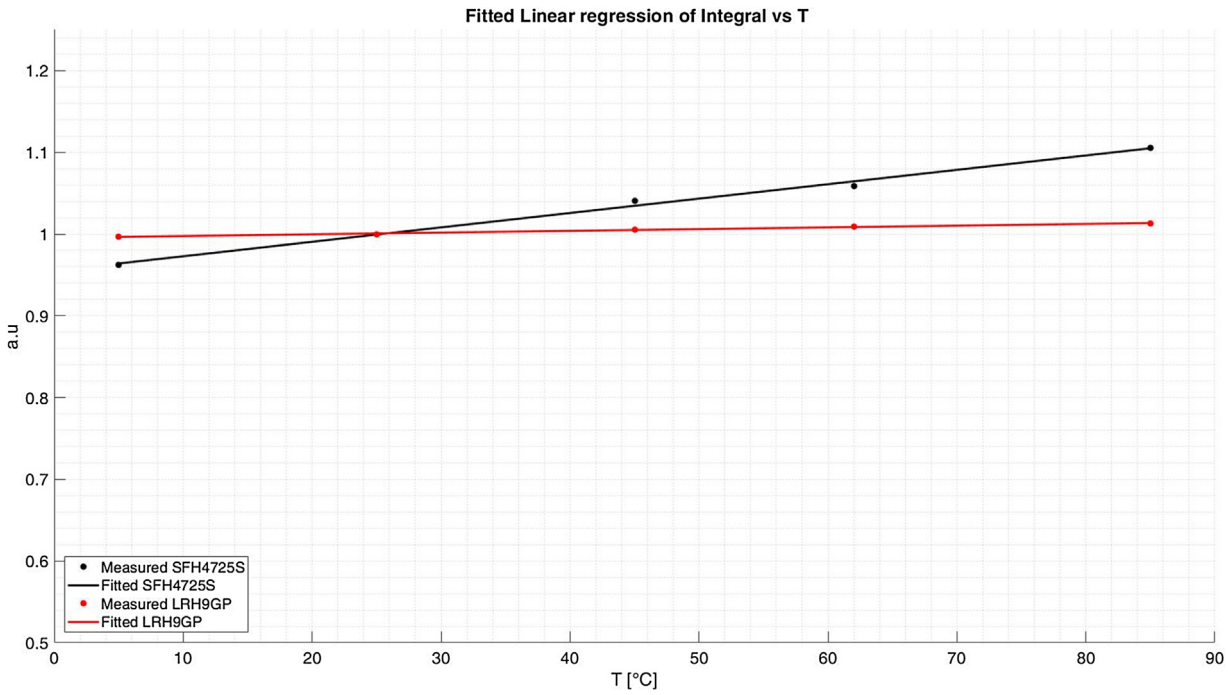

Fig. 6. Representation of measured ratio of integrals of the product between power absorption spectrum of each LED and power spectra of source N.1.e N.2 respectively, as temperature function. The linear curves, which fit measured values are represented by means of solid lines.

Also let:

$$\Gamma_{Integ}(T) = \frac{h_2 \int_{\lambda_{min}}^{\lambda_{max}} S(\lambda) k_2(\lambda) S_{LED}(\lambda, T)\, d\lambda}{h_1 \int_{\lambda_{min}}^{\lambda_{max}} S(\lambda) k_1(\lambda) S_{LED}(\lambda, T)\, d\lambda} \tag{12}$$

ratio of integrals of the product between power absorption spectrum of each LED and power spectra of source N.1.e N.2 respectively, as temperature function.

By normalizing this function in respect of the integrals measured at T_{ref}, it is obtained:

$$\Gamma_{NInteg}(T) = \frac{\dfrac{\int_{\lambda_{min}}^{\lambda_{max}} S(\lambda) k_2(\lambda) S_{LED}(\lambda, T)\, d\lambda}{\int_{\lambda_{min}}^{\lambda_{max}} S(\lambda) k_2(\lambda) S_{LED}(\lambda, T_{ref})\, d\lambda}}{\dfrac{\int_{\lambda_{min}}^{\lambda_{max}} S(\lambda) k_1(\lambda) S_{LED}(\lambda, T)\, d\lambda}{\int_{\lambda_{min}}^{\lambda_{max}} S(\lambda) k_1(\lambda) S_{LED}(\lambda, T_{ref})\, d\lambda}} \tag{13}$$

It follows, from (9) that:

$$\Gamma_{NIsc}(T) = \Gamma_{NInteg}(T) \tag{14}$$

or:

$$\Gamma_{Isc}(T) = \frac{I_{SC2}(T_{ref})}{I_{SC1}(T_{ref})} \Gamma_{NInteg}(T) \tag{15}$$

Consequently, if the source power spectra and LED absorption power spectrum vs. temperature are known, it is possible to extrapolate the function $\Gamma_{Isc}(T)$ and estimate the temperature junction by measuring the ratio of the short circuit currents.

By means of a linear regression interpolation which has taken into account the measured values of the ratio of the product's integrals between each LED absorption spectrum and Source N.1 and Source N.2 spectrum respectively, the obtained functions $\Gamma_{NInteg}(T)$ are represented in Fig. 6.

As to LRH9GP, the function dynamics is very small, whereas when it comes to SFH 4725S, it is wider, which is also expected according to the outcomes shown in Table 1.

Table 2
Comparison between measured junction temperature values and estimated junction temperature ones that have been extrapolated from the function of the ratio between the normalized integrals of the product of each LED absorption spectrum and source N.1 and source N.2 spectrum respectively.

T MEASURED (°C)	T ESTIMATED			
	SFH4725S (°C)	Δ (°C)	LRH9GP (°C)	Δ (°C)
5	5.1	+0.1	6.1	+1.1
25	25.2	+0.2	22.8	−2.2
45	44.2	−0.8	71.2	+26.2
65	66.2	+1.2	79.7	+14.7
85	85.1	+0.1	85.1	+0.1

Δ: difference between estimated temperature and measured temperature.

Figure 7 shows the calculated functions $\Gamma_{NIsc}(T)$ and $\Gamma_{NInteg}(T)$ and you can observe that they display a good overlapping.

Besides, the data collected in Table 2 have been obtained by extracting the junction temperature values from the estimated functions $\Gamma_{NInteg}(T)$ of each DUT.

As to SFH4725S, the estimated temperature values are correlated to the measured ones with the maximum difference (Δ) of 1.2 °C, while, in the other case, the Δ exhibits some larger range variation (up to Δ = 26.2 °C for LRH9GP). This higher error estimation may be due to the very lower angular coefficient of the fitted linear function $\Gamma_{NInteg}(T)$, which depends on the ratio variation of the integrals with respect to the analysed temperature range, as it can be inferred from Eq. (13). On such grounds, it becomes necessary to increase this ratio, in order to achieve higher accuracy in estimating temperature values.

4. Discussion

In this study, due to the use of LEDs as bandwidth-limited photodetectors, the generated photocurrent changes as a temperature function have been correlated with the modifications of mutual overlapping between source and absorption spectra. To correlate the spectral characteristics to the electrical ones, two parameters

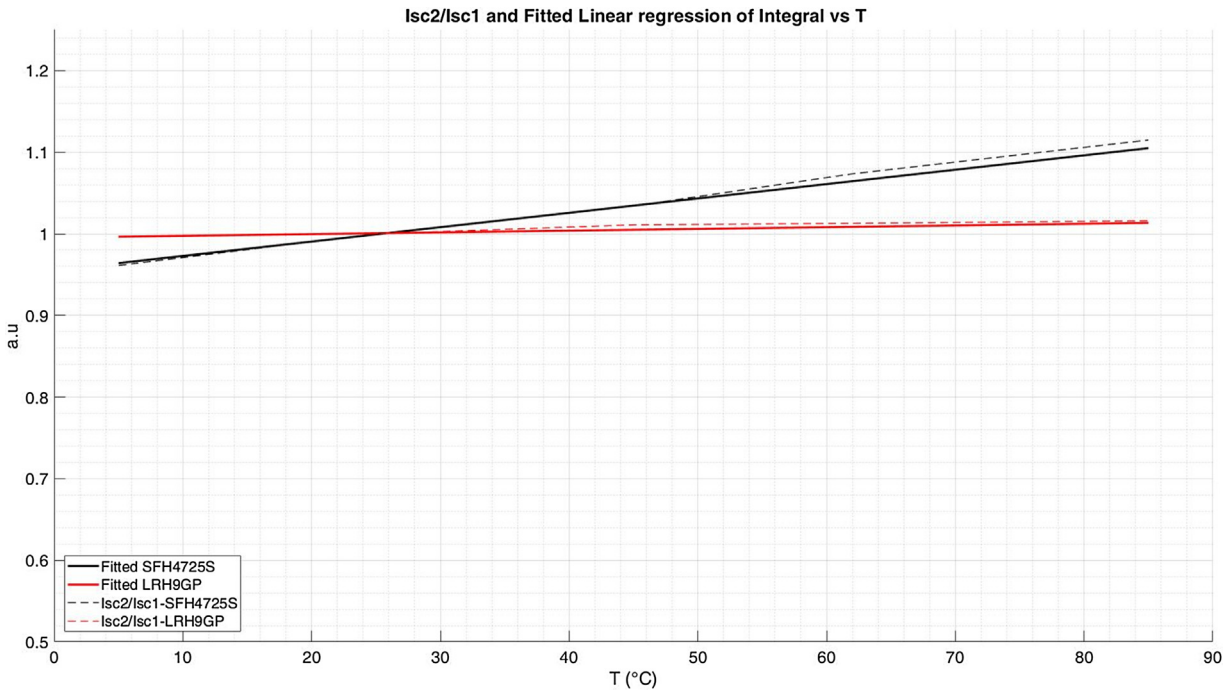

Fig. 7. Comparison between fitted curves of integrals and ratio I_{sc2} to I_{sc1} functions vs temperature for each DUT.

have been defined: the ratio R_{scc}, which takes into account the I_{sc} changes as the temperature varies from value T_1 to T_2 and the ratio R_{sp}, which takes into account the variations of the area of the product between the source and absorption spectra, as long as temperature changes. By comparing their values, as reported in Table 1, it is possible to detect their congruence except for small errors. Therefore, it is possible to assert that the I_{sc} is strongly affected by the spectral characteristics of both the device and the source. The value of the latter, for a specific temperature, can be estimated by measuring the value of R_{sp}. Indeed, the photogenerated current is directly proportional to the area of the product between the spectral power distribution of the source (S_i) and the absorption spectrum of the receiver (S_{LED}).

Wherever observing the I–V characteristics of the analysed LEDs, which is reported in Figs. 3 and 4, a different behaviour comes to light for LED SFH4725S whether sources N.1 or N.2 are used. Indeed, with source N.1 I_{sc} is reduced, instead of increasing as temperature grows. This is caused by some difference in overlapping and, thus, it is due to the different areas of the product between the source and absorption spectra, as shown in Fig. 8.

In this work a mathematical relation, able to describe this behaviour has been proposed and tested starting from the spectral characteristics.

One interesting application, which may result from our study, is about a LED's junction temperature estimation, which can be performed by measuring the ratio between the short circuit photocurrents obtained with two different sources. It should be mentioned that an accurate temperature estimation depends on the $\Gamma_{NInteg}(T)$ dynamics which can be amplified according to the choice of the two concerned sources. Both source spectra are independent from temperature variations, while the absorption spectra increase, shift and enlarge towards higher wavelengths, as temperature increases. Consequently, the range where the absorption spectrum of each LED is overlapped with the source spectra undergoes shifts and the integral of the spectra product changes accordingly. In particular, the more the integral with the first source increases and the more the integral with the second source decreases, the more $\Gamma_{NInteg}(T)$ grows, which is exactly what has occurred with LED SFH 4725S, whose temperature estimation has provided better results than the other LED.

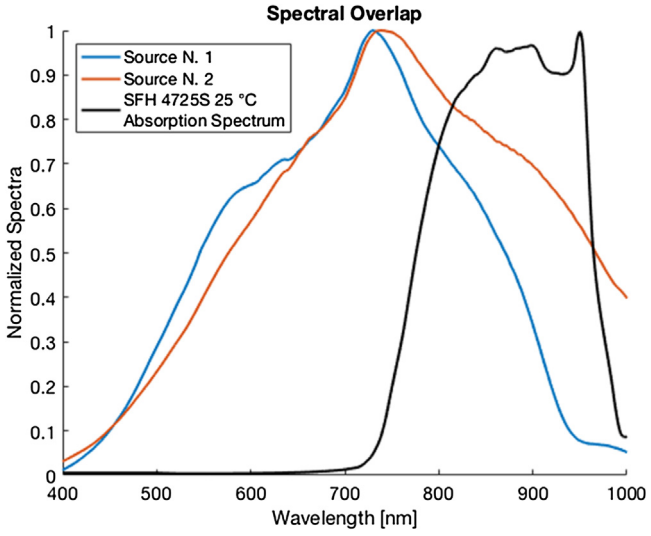

Fig. 8. Different overlaps, at temperature of 25 °C, between SFH 4725S, absorption sectrum and source N.1 and source N.2 emission spectrum, respectively.

An efficient solution may be based on choosing a source having a spectrum represented by an ascending curve as the first source, while the second source should be represented by a descending into the wavelength range covered by the absorption spectrum, as temperature increases. In Fig. 9 an example of a possible sources choice is reported, where $S_1(\lambda)$ and $S_2(\lambda)$ are obtained by filtering a large bandwidth source $S(\lambda)$.

Considerations arisen from the results can extend their scope of activities to include generic photo-detectors and more important information in photovoltaic field can be added. In particular, it may be useful to estimate the temperature value, regardless of the intensity K of the illumination source $S(\lambda)$ (i.e., the sun), as it has been proposed herein. Once the sun spectral power distribu-

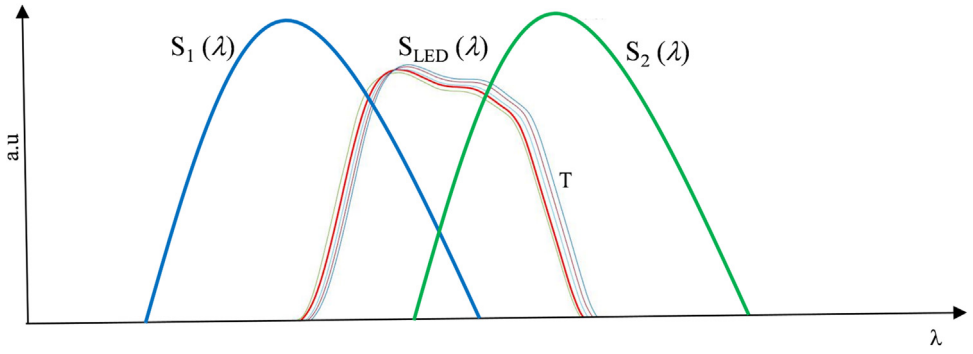

Fig. 9. Example of a couple of illumination sources [$S_1(\lambda)$, $S_2(\lambda)$] choice in respect of the LED absorption spectrum [$S_{LED}(\lambda)$].

tion is undisputed, it may be enough to measure the ratio between the short circuit currents, photogenerated by illuminating the solar cell with two different optical filters having appropriate spectral characteristics.

On the other hand, an investigation on a larger wavelength domain may increase knowledge not only in photovoltaic applications, requiring a wavelength range up to 1200 nm at least, but with different types of LEDs characterization as photoreceptors, as well. In fact, the bibliography attached to this paper clearly speaks of an emerging interest in employing LEDs as photoreceptors within several applications. Therefore, having a better interpretation of the phenomena causing the short circuit current variations, may be of help in improving the device performances in terms of signal-to-noise ratio and sensitivity.

5. Conclusions

In this work, a novel procedure to estimate LED junction temperature has been presented on the basis of spectral and electrical characteristics of different LEDs in the wavelength range of 400–1000 nm, at five temperature levels (5 °C, 25 °C, 45 °C, 65 °C, 85 °C) and by using two different light sources.

The method is based on the knowledge of both two source spectral distributions and the DUT absorption spectrum temperature behaviour, which allows for the relationship between short circuit photocurrents ratio and temperature. A mathematical analysis has been proposed and tested with experimental results in order to highlight the independence of the proposed method from the intensity of the illumination source. A more extensive experimentation is required to confirm and improve the results that can be exploited within generic photo-detector field and in the photovoltaic field, as well.

Acknowledgement

We thank the Power Control s.r.l (Pisa, Italy) for the important technical support and collaboration in this demanding experimental work.

References

[1] E. Radziemska, E. Klugmann, Thermally affected parameters of the current–voltage characteristics of silicon photocell, Energy Convers. Manag. 43 (2002) 1889–1900, http://dx.doi.org/10.1016/S0196-8904(01)00132-7.
[2] P. Singh, N.M. Ravindra, Temperature dependence of solar cell performance—an analysis, Sol. Energy Mater. Sol. Cells 101 (2012) 36–45, http://dx.doi.org/10.1016/j.solmat.2012.02.019.
[3] S. Chander, A. Purohit, A. Sharma, S.P. Nehra, M.S. Dhaka, Impact of temperature on performance of series and parallel connected mono-crystalline silicon solar cells, Energy Rep. 1 (2015) 175–180, http://dx.doi.org/10.1016/j.egyr.2015.09.001.
[4] Y.P. Varshni, Temperature dependence of the energy gap in semiconductors, Physica 34 (1967) 149–154, http://dx.doi.org/10.1016/0031-8914(67)90062-6.
[5] Y. Xi, E.F. Schubert, Junction–temperature measurement in GaN ultraviolet light-emitting diodes using diode forward voltage method, Appl. Phys. Lett. 85 (2004) 2163–2165, http://dx.doi.org/10.1063/1.1795351.
[6] S. Chhajed, Y. Xi, Y.-L. Li, T. Gessmann, E.F. Schubert, Influence of junction temperature on chromaticity and color-rendering properties of trichromatic white-light sources based on light-emitting diodes, J. Appl. Phys. 97 (2005) 054506, http://dx.doi.org/10.1063/1.1852073.
[7] Y. Xi, J.-Q. Xi, T. Gessmann, J.M. Shah, J.K. Kim, E.F. Schubert, A.J. Fischer, M.H. Crawford, K.H.A. Bogart, A.A. Allerman, Junction and carrier temperature measurements in deep-ultraviolet light-emitting diodes using three different methods, Appl. Phys. Lett. 86 (2005) 031907, http://dx.doi.org/10.1063/1.1849838.
[8] E.E. Perl, J. Simon, J.F. Geisz, M.L. Lee, D.J. Friedman, M.A. Steiner, Measurements and modeling of III-V solar cells at high temperatures up to 400 $ĉirc$C, IEEE J. Photovolt. 6 (2016) 1345–1352, http://dx.doi.org/10.1109/JPHOTOV.2016.2582398.
[9] C.R. Osterwald, Translation of device performance measurements to reference conditions, Sol. Cells 18 (1986) 269–279, http://dx.doi.org/10.1016/0379-6787(86)90126-2.
[10] K. Emery, C. Osterwald, Measurement of photovoltaic device current as a function of voltage, temperature, intensity and spectrum, Sol. Cells 21 (1987) 313–327, http://dx.doi.org/10.1016/0379-6787(87)90130-X.
[11] H.J. Hovel, R.K. Willardson, A.C. Beer, Semiconductors and Semimetals, Vol. 11, Academic Press, New York, 1975, Vol. 11.
[12] A.L. Fahrenbruch, R.H. Bube, Chapter 4 - application of the transport equation, in: Fundam. Sol. Cells, Academic Press, 1983, pp. 69–104, http://dx.doi.org/10.1016/B978-0-12-247680-8.50010-4.
[13] K.P. O'Donnell, X. Chen, Temperature dependence of semiconductor band gaps, Appl. Phys. Lett. 58 (1991) 2924–2926, http://dx.doi.org/10.1063/1.104723.
[14] K.-C. Chiu, Y.-C. Su, H.-A. Tu, Fit of temperature dependence of semiconductor band gaps, Jpn. J. Appl. Phys. 37 (1998) 6374–6375, http://dx.doi.org/10.1143/JJAP.37.6374.
[15] E. Miyazaki, S. Itami, T. Araki, Using a light-emitting diode as a high-speed, wavelength selective photodetector, Rev. Sci. Instrum. 69 (1998) 3751–3754, http://dx.doi.org/10.1063/1.1149174.
[16] R. Filippo, E. Taralli, M. Rajteri, L.E.Ds: Sources, Intrinsically bandwidth-limited detectors, Sensors 17 (2017) 1673, http://dx.doi.org/10.3390/s17071673.
[17] M. Kowalczyk, J. Siuzdak, Photo-reception properties of common LEDs, Opto-Electron. Rev. 25 (2017) 222–228, http://dx.doi.org/10.1016/j.opelre.2017.06.009.
[18] D.A. Lock, S.R.G. Hall, A.D. Prins, B.G. Crutchley, S. Kynaston, S.J. Sweeney, L.E.D. Junction Temperature, Measurement using generated photocurrent, J. Disp. Technol. 9 (2013) 396–401, http://dx.doi.org/10.1109/JDT.2013.2251607.
[19] F. Yang, M. Wilkinson, E.J. Austin, K.P. O'Donnell, Origin of the Stokes shift: a geometrical model of exciton spectra in 2D semiconductors, Phys. Rev. Lett. 70 (1993) 323–326, http://dx.doi.org/10.1103/PhysRevLett.70.323.
[20] R.W. Martin, P.G. Middleton, K.P. O'Donnell, W. Van der Stricht, Exciton localization and the Stokes' shift in InGaN epilayers, Appl. Phys. Lett. 74 (1999) 263–265, http://dx.doi.org/10.1063/1.123275.
[21] K.P. O'Donnell, R.W. Martin, P.G. Middleton, Origin of Luminescence from InGaN diodes, Phys. Rev. Lett. 82 (1999) 237–240, http://dx.doi.org/10.1103/PhysRevLett.82.237.
[22] Journal of the Korean Physical Society, Springer.Com (n.d.). http://www.springer.com/physics/journal/40042 (Accessed 29 September 2017).
[23] F.M. Mims, Sun photometer with light-emitting diodes as spectrally selective detectors, Appl. Opt. 31 (1992) 6965–6967, http://dx.doi.org/10.1364/AO.31.006965.
[24] Y.B. Acharya, A. Jayaraman, S. Ramachandran, B.H. Subbaraya, Compact light-emitting-diode sun photometer for atmospheric optical depth measurements, Appl. Opt. 34 (1995) 1209–1214.

[25] D.R. Brooks, F.M. Mims, Development of an inexpensive handheld LED-based Sun photometer for the GLOBE program, J. Geophys. Res. Atmosp. 106 (2001) 4733–4740, http://dx.doi.org/10.1029/2000JD900545.
[26] F.M. Mims, An inexpensive and stable LED Sun photometer for measuring the water vapor column over South Texas from 1990 to 2001, Geophys. Res. Lett. 29 (2002) 20–21, http://dx.doi.org/10.1029/2002GL014776.
[27] Y.B. Acharya, Spectral and emission characteristics of LED and its application to LED-based sun-photometry, Opt. Laser Technol. 37 (2005) 547–550, http://dx.doi.org/10.1016/j.optlastec.2004.08.008.
[28] J. Rossiter, T. Mukai, A novel tactile sensor using a matrix of LEDs operating in both photoemitter and photodetector modes, IEEE Sens. 2005 (2005) 4, http://dx.doi.org/10.1109/ICSENS.2005.1597869.
[29] K. Okamoto, Intelligent non-conventional applications of LEDs, Trans. Jpn. Inst. Electron. Packag. 3 (2010) 116–123, http://dx.doi.org/10.5104/jiepeng.3.116.
[30] C. Weber, J.O. Tocho, E.J. Rodríguez, H.A. Acciaresi, Leds used as spectral selective light detectors in remote sensing techniques, J. Phys. Conf. Ser. 274 (2011) 012103, http://dx.doi.org/10.1088/1742-6596/274/1/012103.
[31] D.-Y. Shin, J.Y. Kim, I.-Y. Eom, Spectral responses of light-emitting diodes as a photodiode and their applications in optical measurements, Bull. Korean Chem. Soc. 37 (2016) 2041–2046, http://dx.doi.org/10.1002/bkcs.11030.
[32] S. Li, A. Pandharipande, F.M.J. Willems, Daylight sensing LED lighting system, IEEE Sens. J. 16 (2016) 3216–3223, http://dx.doi.org/10.1109/JSEN.2016.2520495.
[33] V. Lange, F. Lima, D. Kühlke, Multicolour LED in luminescence sensing application, Sens. Actuators Phys. 169 (2011) 43–48, http://dx.doi.org/10.1016/j.sna.2011.05.002.
[34] S. Li, A. Pandharipande, Color sensing and illumination with LED lamps, in: 2014 IEEE fourth int, Conf. Consum. Electron. Berl. ICCE-Berl. (2014) 1–2, http://dx.doi.org/10.1109/ICCE-Berlin.2014.7034294.
[35] S. Li, A. Pandharipande, LED-based color sensing and control, IEEE Sens. J. 15 (2015) 6116–6124, http://dx.doi.org/10.1109/JSEN.2015.2453408.
[36] M. O'Toole, D. Diamond, Absorbance based light emitting diode optical, Sens. Sens. Devices, Sens. 8 (2008) 2453–2479, http://dx.doi.org/10.3390/s8042453.
[37] R. Stojanovic, D. Karadaglic, Design of an oximeter based on LED-LED configuration and FPGA technology, Sensors 13 (2013) 574–586, http://dx.doi.org/10.3390/s130100574.
[38] E. Taralli, R. Filippo, G. Brida, M. Rajteri, S.R.G. Hall, A. Bialek, C. Greenwell, N. Fox, LED-based field radiometer for sensor web in-situ measurements, in: 2015 IEEE Metrol. Aerosp. MetroAeroSpace, 2015, pp. 318–322, http://dx.doi.org/10.1109/MetroAeroSpace.2015.7180675.
[39] J.S. Czapla-Myers, K.J. Thome, S.F. Biggar, Design, calibration, and characterization of a field radiometer using light-emitting diodes as detectors, Appl. Opt. 47 (2008) 6753–6762.
[40] B. Wu, S. Lin, T.M. Shih, Y. Gao, Y. Lu, L. Zhu, G. Chen, Z. Chen, Junction-temperature determination in InGaN light-emitting diodes using reverse current method, IEEE Trans. Electron. Devices 60 (2013) 241–245, http://dx.doi.org/10.1109/TED.2012.2228656.